Immune Netw. 2024 Oct;24(5):e37
https://doi.org/10.4110/in.2024.24.e37
pISSN 1598-2629·eISSN 2092-6685

IMMUNE NETWORK

Original Article

STING-STAT6 Signaling Pathway Promotes IL-4$^+$ and IFN-α^+ Fibrotic T Cell Activation and Exacerbates Scleroderma in SKG Mice

Kun Hee Lee [1,2], **Jin Seok Woo** [1], **Ha Yeon Jeong**[1,2], **Jeong Won Choi** [1,2], **Chul Hwan Bang**[3], **Jeehee Youn**[4], **Sung-Hwan Park**[5,*], **Mi-La Cho** [1,2,6,*]

[1]Lab of Translational ImmunoMedicine, Catholic Research Institute of Medical Science, College of Medicine, The Catholic University of Korea, Seoul 06591, Korea
[2]Department of Pathology, College of Medicine, The Catholic University of Korea, Seoul 06591, Korea
[3]Department of Dermatology, Seoul St. Mary's Hospital, College of Medicine, The Catholic University of Korea, Seoul 06591, Korea
[4]Department of Anatomy & Cell Biology, College of Medicine, Hanyang University, Seoul 04763, Korea
[5]Division of Rheumatology, Department of Internal Medicine, Seoul St. Mary's Hospital, College of Medicine, The Catholic University of Korea, Seoul 06591, Korea
[6]Department of Biomedicine & Health Sciences, College of Medicine, The Catholic University of Korea, Seoul 06591, Korea

Received: Nov 28, 2023
Revised: Sep 21, 2024
Accepted: Sep 25, 2024
Published online: Oct 16, 2024

***Correspondence to**
Sung-Hwan Park
Division of Rheumatology, Department of Internal Medicine, Seoul St. Mary's Hospital, College of Medicine, The Catholic University of Korea, 222 Banpo-daero, Seocho-gu, Seoul 06591, Korea.
Email: rapark@catholic.ac.kr

Mi-La Cho
Department of Pathology, College of Medicine, The Catholic University of Korea, 222 Banpo-daero, Seocho-gu, Seoul 06591, Korea.
Email: iammila@catholic.ac.kr

ORCID iDs
Kun Hee Lee
https://orcid.org/0009-0000-6773-7670
Jin Seok Woo
https://orcid.org/0000-0001-8921-2832
Jeong Won Choi
https://orcid.org/0000-0003-4299-7155
Mi-La Cho
https://orcid.org/0000-0001-5715-3989

ABSTRACT

Systemic sclerosis (SS) is an autoimmune disease and pathological mechanisms of SS are unclear. In this study, we investigated the role of T cells in the progression of SS using SKG mice and humanized mice. SKG mice have a spontaneous point mutation in ZAP70. We induced scleroderma in SKG mice and a humanized SS mouse model to assess whether T cell-mediated immune responses induce SS. As a result, we found increased dermal thickness, fibrosis, and lymphocyte infiltration in skin tissue in SKG SS mice compared to BALB/c mice (control). Also, blood cytokine level, including IL-4- and IFN-α which are produced by CD4$^+$ T cells via STIM1/STING/STAT6/IRF3 signaling pathways, were increased in SKG mice. Interestingly, skin fibrosis was reduced by inhibiting STING pathway in skin fibroblast. Next, we demonstrated the pathophysiological role of IL-4 and IFN-α in skin fibrosis using a humanized SS mouse model and found increased IL-4- and IFN-α-producing CD4$^+$ T cells and fibrosis. In this study, we found that STING-induced production of IL-4- and type I IFN by CD4$^+$ T cells is a key factor in mouse model and humanized mouse model of SS. Our findings suggest that the STING/STAT6/IRF3 signaling pathways are potential therapeutic targets in SS.

Keywords: Systemic sclerosis; T cell; STING; STAT6 transcription factor; Cytokine

INTRODUCTION

Scleroderma, also known as systemic sclerosis (SS), is an autoimmune disease characterized by thickening of the skin, fibrosis, and vasculopathy (1). The pathological mechanisms of SS are unclear; however, pro-inflammatory cytokines and the tissue microenvironment are important in its development (2,3).

IMMUNE NETWORK

Conflict of Interest
The authors declare no potential conflicts of interest.

Abbreviations
α-SMA, α-smooth muscle actin; BLM, bleomycin; cGAMP, cyclic guanosine monophosphate-adenosine monophosphate; CTGF, connective tissue growth factor; DC, dendritic cell; ER, endoplasmic reticulum; GM130, Golgi matrix protein 130; IRF3, Interferon regulatory factor 3; MT, Masson's trichrome; PBMC, peripheral blood mononuclear cell; PM, plasma membrane; SOCE, store-operated Ca2+ entry; SS, systemic sclerosis; STAT6, signal transducer and activator of transcription 6; STIM1, stromal interaction molecule 1; STING, stimulator of interferon genes; TBK1, TANK-binding kinase 1; TCR, T-cell receptor; ZAP70, z chain-associated protein 70.

Data Availability
All datasets generated for this study are included in the article.

Author Contributions
Conceptualization: Lee KH, Cho ML; Data curation: Lee KH; Formal analysis: Lee KH; Investigation: Lee KH, Woo JS; Methodology: Lee KH, Woo JS, Jeong HY, Choi JW; Resources: Youn J, Park SH; Software: Lee KH, Woo JS; Validation: Lee KH, Woo JS; Writing - original draft: Lee KH, Woo JS; Writing - review & editing: Bang CH, Park SH, Cho ML.

Collagen, the main effector molecule in SS, is more abundant in skin with mononuclear cell infiltration (4). Inflammatory cytokines secreted by immune cells enhance the deposition of collagen (5). The levels of Th cells that produce IL-4 (Th2) and IL-17 (Th17) are increased in skin and blood in SS (6-8). However, IL-17A in SS patients may induce inflammatory responses while protecting against fibrosis (9).

Calcium (Ca^{2+}) signaling plays an important role in the regulation of the immune system (10). Store-operated Ca^{2+} entry (SOCE) is a major Ca^{2+} signaling pathway in the immune system. It is regulated by stromal interaction molecule 1 (STIM1) and acts as a Ca^{2+} sensor at the endoplasmic reticulum (ER) membrane. Activated STIM1 translocates from the ER membrane to the plasma membrane (PM) and interacts with Calcium release-activated calcium channel protein 1 (ORAI1), which acts as a Ca^{2+} channel at PM (11). STIM1 also regulates the activity of stimulator of interferon genes (STING) (12), an ER-resident protein upstream of type I IFN production in myeloid cells (13,14). DNA-bound cGAS produces a cyclic dinucleotide, 2′,3′-cyclic guanosine monophosphate–adenosine monophosphate (cGAMP), which is a STING ligand (15). cGAMP provokes translocation of STING from the ER to the ER-Golgi compartment, recruiting TANK-binding kinase 1 (TBK1) (16). Interferon regulatory factor 3 (IRF3) and signal transducer and activator of transcription 6 (STAT6) (17,18), which are transcription factors that induce type I IFN and IL-4, respectively, are phosphorylated and translocate to the nucleus to produce type I IFN and IL-4 (19,20).

The SKG mouse has a point mutation of the gene encoding TCR–z chain-associated protein 70 (ZAP70), a key molecule in signal transduction in T cells, and develops spontaneous chronic autoimmune arthritis (21,22). The expression of IL-1, TNF-α, and IL-6 is increased in arthritic SKG mice (23). Thus, external stimuli may trigger autoimmune diseases in SKG mice by stimulating autoimmune T cells.

To assess the role of T cells in SS, SKG mice were subcutaneously injected with bleomycin (BLM). Next, we evaluated whether BLM-treated SKG mice exhibited more of the SS phenotype than BLM-treated BALB/c, and if so, determined the underlying molecular mechanisms. We investigated whether the STIM1-STING pathway is activated in $CD4^+$ T cells in BLM-treated SKG mice. We also explored whether IL-4- and IFN-α-producing $CD4^+$ T cells exist by increase in phospho-STAT6 (pSTAT6) and phospho-IRF3 (pIRF3) and whether skin fibrosis is induced by these cytokines. Finally, we confirmed that inhibition of STING-STAT6 pathway decreased IL-4- and IFN-α-producing $CD4^+$ T cells and suppressed skin fibrosis.

MATERIALS AND METHODS

Animals

Eight-week-old BALB/c and SKG male mice were used. BALB/c mice were purchased from OrientBio (Seongnam, Korea) and SKG mice were from Saeronbio (Uiwang, Korea). Seven-week-old NOD/scid/IL-2Rγ$^{-/-}$ female mice (NOD.Cg-Prkdc^{scid}IL2rg^{tm1Wjl}/SzJ; NSG) were obtained from The Jackson Laboratory (Bar Harbor, ME, USA). They were fed standard mouse chow (Ralston Purina, St. Louis, MO, USA) and water ad libitum. Experimental procedures were reviewed and approved by the Animal Research Ethics Committee of the Catholic University of Korea (Seoul, Korea).

https://doi.org/10.4110/in.2024.24.e37

BLM, H-151 and AS1517499 treatment

The mice were anesthetized with isoflurane, and their backs were shaved. They were given daily subcutaneous injections of 0.5 mg/ml BLM in 100 μl for 2 wk (Dong-A Pharm, Seoul, Korea). They were euthanized 3 weeks after the final BLM treatment. Back skin tissue was fixed in 10% formalin for histological analysis. Spleen tissue was embedded in Optimal Cutting Temperature Compound (LEICA, 3801480) for cryosectioning. H-151 (1 or 10 mg/kg) in 10% DMSO/40% PEG300/5% Tween-80/45% Saline was injected intraperitoneally three times a week for 3 wk after the final injection of BLM. AS1517499 (10 mg/kg) in 20% DMSO in saline was subcutaneously injected three times a week for 3 weeks after the final injection of BLM.

Histological assessment

Harvested tissue was fixed in 10% formalin and embedded in paraffin. The tissue was sliced at 5 μm thickness and placed on standard microscopy slides. Sections were stained with Hematoxylin & Eosin and Masson's trichrome (MT). MT staining was conducted using the Trichrome Stain (Masson) Kit (HT15, Sigma-Aldrich, St. Louis, MO, USA). After deparaffinization and rehydration, the slides were immersed in Bouin's solution (HT 10132, Sigma-Aldrich) at 56°C for 1 h. Subsequently, the slides were washed with tap water for 5 min. Next, the tissues were stained with Weigert's hematoxylin for 5 min, and washed with tap water for 5 min. The slides were stained in Biebrich scarlet-acid fuchsin for 5 min, rinsed in distilled water, incubated in phosphotungstic-phosphomolybdic acid for 5 min, dyed with aniline blue for 5 min, and fixed in 1% acetic acid for 2 min. Finally, the slides were washed in distilled water, dehydrated, and mounted. Dermal thickness was measured as described previously.

Immunohistochemistry

Harvested tissue was fixed in 10% formalin and embedded in paraffin. The tissue was sliced at 5 μm thickness and placed on standard microscopy slides. Immunohistochemistry was performed using the Vectastain ABC Kit (Vector Laboratories, Burlingame, CA, USA). Tissue was incubated with primary Abs against α-smooth muscle actin (α-SMA), collagen 1, IL-1β, IL-6, TNFα, IL-4, IL-17, phospho-STING, phospho-IRF3, phospho-STAT6, and IFNα overnight at 4°C. The primary Abs were detected using a biotinylated secondary Ab, followed by incubation with streptavidin-peroxidase complex for 30 min. The final color was produced using DAB chromogen (Dako, Carpinteria, CA, USA). Stained cells, which were identified according to a dark brown deposit in the nucleus, were enumerated in three randomly selected high-power fields (HPFs; 400×; 2.37 mm^2). The sections were counterstained with hematoxylin and photographed with an Olympus photomicroscope (Tokyo, Japan).

Flow cytometry

Cells were isolated from the spleens of BALB/c and SKG mice. Prior to staining, cells were stimulated for 3 days with LPS (1 μg/ml) and treated for 4 h with Golgistop (BD Biosciences, San Jose, CA, USA). The cells were surface-stained with PerCP-conjugated anti-CD4 Abs (eBioscience). Then these cells were permeabilized using Cytofix/Cytoperm solution (BD Pharmingen, Franklin Lakes, NJ, USA), and subjected to intracellular staining using PE-conjugated anti-IL-4 (BD Biosciences), APC-conjugated anti-IL-17 (eBioscience), FITC-conjugated anti-IFNα (R&D Systems Minneapolis, MN, USA), anti-phosphor STING (Invitrogen, Waltham, MA, USA), anti-phosphor IRF3 (Cell Signaling Technology, Danvers, MA, USA), and anti-phosphor STAT6 (Santa Cruz Biotechnology, Dallas, TX, USA) Abs. Next, anti-phosphor STING, anti-phosphor IRF3, and anti-phosphor STAT6 were detected using an Efluor 450-conjugated secondary Ab (Invitrogen) or APC-conjugated secondary Ab (BD Biosciences). Flow cytometry was performed on a cytoFLEX Flow Cytometer (Beckman

Coulter, Brea, CA, USA) and data were analyzed using FlowJo software (Tree Star, Ashland, OR, USA).

T-cell differentiation

Splenocytes were acquired from spleen tissues of BALB/c mice and SKG mice and sieved through a mesh screen. Next, red blood cells were lysed in hypotonic ACK buffer. The remaining splenocytes were maintained in RPMI 1640 medium containing 5% fetal bovine serum. Before T cell differentiation, the plate was coated with anti-CD3 (0.5 μg/ml; BD Pharmingen) for 2 h at 37°C. Next, splenocytes were cultured with anti-CD28 (1 μg/ml) Ab, anti-IFN-γ (2 μg/ml) Ab, and IL-4 (10 ng/ml) in the absence or presence of H-151 (0.5 μM; InvivoGen), or AS1517499 (10 μM) for 3 days. Recombinant mouse IL-4 and Abs to CD28 and IFN-γ were purchased from R&D Systems.

Confocal microscopy

Skin tissue sections of 5 μm thickness, spleen tissue sections of 7 μm thickness, splenocytes from spleen tissues of BALB/c and SKG mice, and human skin fibroblasts were used for immunostaining. Splenocytes were attached to standard microscopy slides using Cytospin. We used anti-CD4 (Novus Biologicals, Centennial, CO, USA), anti-IL-4 (Invitrogen), anti-IL-17 (Invitrogen), anti-IFNα (Invitrogen), anti-phosphor STING (Invitrogen), anti-phosphor IRF3 (Cell Signaling), anti-phosphor STAT6 (Invitrogen), anti-GM130 (Santa Cruz Biotechnology), anti-STING (Cell Signaling Technology), anti-STIM1 (Invitrogen), anti-ORAI1 (Invitrogen) Abs, α-SMA and fibronectin (Abcam, Cambridge, UK). Slides were visualized under a microscope (LSM 700; Carl Zeiss, Oberkochen, Germany) at ×200 magnification.

SSc patients and the isolation of PBMCs

Peripheral blood was acquired from healthy controls (HC, n=4) and SS patients (n=3) who visited Seoul St. Mary's Hospital, a tertiary referral hospital in the Republic of Korea. PBMCs were isolated from heparinized blood by Ficoll-Paque density gradient centrifugation.

Humanized scleroderma mouse model

To develop the patient-derived humanized scleroderma mouse model, isolated human PBMCs (5×10^6/mouse) from SS patients were intraperitoneally injected into NSG mice (24). After 2 wk, the mice were anesthetized with isoflurane, and their backs were shaved. They were given daily subcutaneous injections of 25 μg BLM for 4 weeks (Dong-A Pharm, Seoul, Korea). The mice were euthanized after the final treatment. Back skin tissue was fixed in 10% formalin for histological analysis.

Primary skin fibroblast culture

Normal skin tissues from a healthy donor were washed with PBS, cut into small pieces, and adhered to and cultured on the bottoms of tissue culture flasks. After 3 days, primary skin fibroblasts were collected and cultured in Dulbecco's modified Eagle's medium (Gibco, Grand Island, NY, USA) supplemented with 10% FBS (Gibco), containing 100 μg/ml streptomycin and 100 U/ml penicillin, at 37°C in an atmosphere of 5.0% CO_2. Skin fibroblasts were cultured with/without 10 ng/ml IL-4, 1,500 units/ml IFNα, and 0.5 μM H-151 for 1 day. Recombinant human IL-4 and IFNα were purchased from R&D Systems.

https://doi.org/10.4110/in.2024.24.e37

Statistical analysis

Data are presented as means ± SEMs. Statistical analysis was performed using Prism ver. 8 software for Windows (GraphPad Software, San Diego, CA, USA). Normally distributed continuous data were analyzed using the parametric Student's *t*-test. Among-group differences in means were subjected to one-way ANOVA; $p<0.05$ was taken to indicate statistical significance.

Ethics approval

Study procedures involving humans were approved by the Institutional Review Board of the Catholic University of Korea (approval number: KC17TNSI0237). All mice experimental procedures were approved by the Department of Laboratory Animals, Institutional Animal Care and Use Committee (IACUC) of the School of Medicine, the Catholic University of Korea and conformed with all National Institutes of Health (Bethesda, MD, USA) guidelines (Approval number: CUMC-2022-0049-05 and CUMC-2020-0351-04).

RESULTS

Fibrosis and inflammatory cytokines are increased in skin of BLM-treated SKG mice

SKG mice spontaneously develop arthritis. To investigate the role of T cells in SS pathogenesis, we injected BLM into BALB/c and SKG mice for 2 wk (**Fig. 1A**). H&E and MT staining revealed that skin thickness and fibrosis were increased in BLM-treated SKG mice compared to BLM-treated BALB/c mice (**Fig. 1B**). Immunohistochemistry showed that the expressions of α-SMA and Col1 were significantly increased in the skin tissue of BLM-treated SKG mice compared to BLM-treated BALB/c mice (**Fig. 1C**). To assess the effects of T cells on SS, we measured the expression level of inflammatory cytokines of skin tissue via immunohistochemistry. BLM-treated SKG mice had increased expression of inflammatory cytokines, such as IL-1β, IL-6, TNF-α, IL-4, IL-17, and IFN-α (**Fig. 1D**). These data suggest that BLM-induced SS is further developed in SKG mice

Levels of inflammatory cytokines are increased in $CD4^+$ T cells of BLM-treated SKG mice *in vivo* and the STIM1/STING pathway and its STAT6 and IRF3 downstream pathways are activated in $CD4^+$ T cells of SKG mice *in vitro*

Th2 ($CD4^+IL\text{-}4^+$) and Th17 ($CD4^+IL\text{-}17^+$) cells are important in SS. Flow cytometry showed that the number of Th2 ($CD4^+IL\text{-}4^+$) cells was increased among splenocytes in BLM-treated SKG mice compared to BLM-treated BALB/c mice (**Fig. 2A**). The number of Th17(CD4+IL-17+) cells tended to increase in splenocytes from BLM-treated SKG mice compared to splenocytes from BLM-treated BALB/c mice, but this was not statistically significant. Immunofluorescence showed that the numbers of Th2 cells and Th17 cells in spleen tissue were increased in BLM-treated SKG mice (**Fig. 2B**). Activation of TCR signaling by mutation of ZAP70 activates ORAI1 and STIM1, leading to activation of STING. $CD4^+$ T cells from BALB/c and SKG mice were differentiated under Th2-skewing conditions. After differentiation, these cells were stained with Abs against STIM1 and ORAI1 to measure their co-localization at the PM. The results showed that STIM1 translocated to the PM and co-localized with ORAI1 in cells from SKG mice (**Fig. 2C**). In addition, the number of pSTING-producing $CD4^+$ T cells was higher in SKG mice than in BALB/c mice by flow cytometry (**Fig. 2D** and **Supplementary Fig. 1**). Also, the number of $CD4^+$ T cells expressing pSTAT6 and pIRF3, downstream transcription factors of STING, and the number of $CD4^+$ T cells simultaneously expressing IL-4 and IFN-α were

https://doi.org/10.4110/in.2024.24.e37

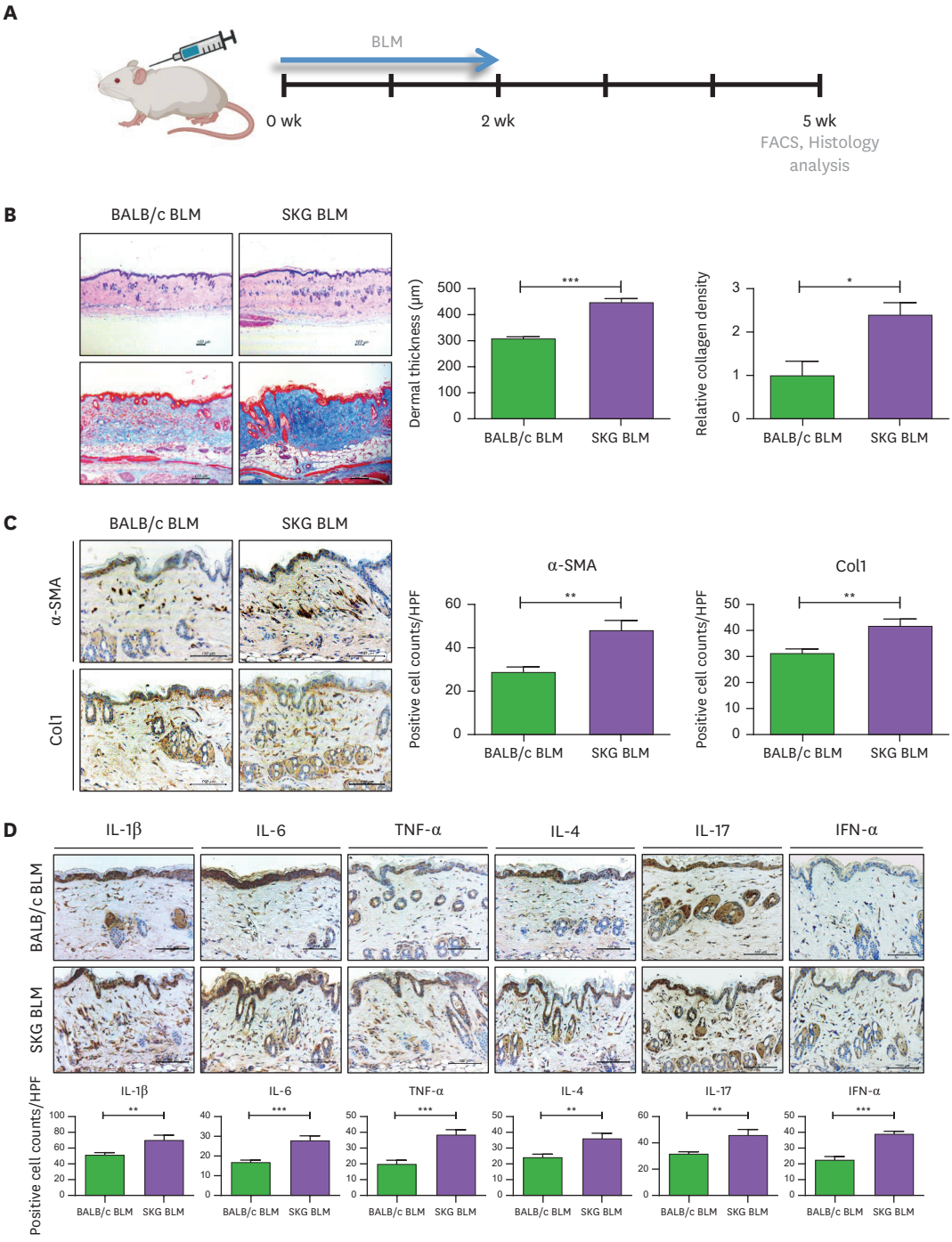

Figure 1. Fibrosis and inflammatory cytokines are increased in skin of BLM-treated SKG mice. (A) Mice were given daily subcutaneous injections of BLM for 2 wk (BLM-treated BALB/c mice [n=5] and SKG mice [n=4]). (B) H&E staining and MT images of dermis thickness and collagen density in skin tissues of BLM-treated mice. Scale bars=100 μm. (C) Representative α-SMA and Col1-stained images of skin tissues of BLM-treated mice. Scale bars=100 μm. (D) Immunohistochemistry for IL-1β, IL-6, TNF-α, IL-4, IL-17, and IFN-α in skin tissues of BLM-treated mice. Scale bars=100 μm. Values are means ± SEMs from three independent experiments. BLM, bleomycin.
*p<0.05, **p<0.01, and ***p<0.001.

evaluated by flow cytometry (**Fig. 2D** and **Supplementary Fig. 1**). Therefore, autoimmune T cells of SKG mice were increased the STIM1/STING pathway, resulting in T cells co-expressing IL-4 and IFN-α.

https://doi.org/10.4110/in.2024.24.e37

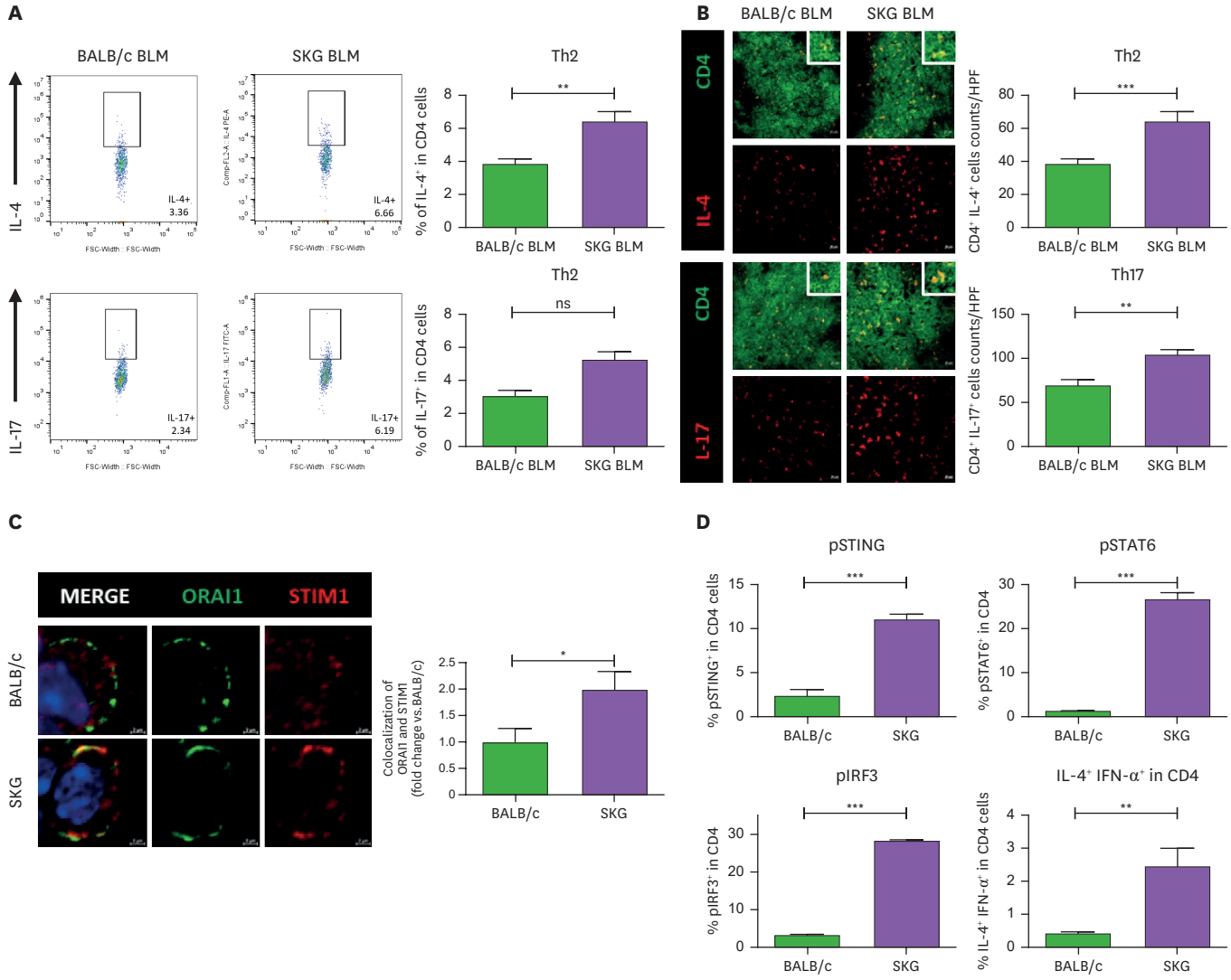

Figure 2. Levels of inflammatory cytokines are increased in CD4⁺ T cells of BLM-treated SKG mice *in vivo* and the STIM1/STING pathway and its STAT6 and IRF3 downstream pathways are activated in CD4⁺ T cells of SKG mice *in vitro*. (A) Numbers of CD4⁺IL-4⁺ (Th2) and CD4⁺IL-17⁺ (Th17) cells in spleens of BLM-treated mice (n=3 per group). Cells were stimulated with LPS for 3 days and Golgistop for the final 4 h. (B) Spleen tissues of BLM-treated mice were stained with anti-CD4 (green), anti-IL-4 (red), and anti-IL-17 (red) Abs to identify Th2 and Th17 cells (BLM-treated BALB/c mice [n=5] and SKG mice [n=4]). Scale bars=20 μm. (C) CD4⁺ T cells from spleen tissues of mice were stained with anti-ORAI1 (green) and anti-STIM1 (red) Abs. Scale bars=20 μm. (D) Numbers of pSTING⁺ cells, pSTAT6⁺ cells, pIRF3⁺ cells, and IL-4⁺ IFN-α⁺ cells of CD4⁺ T cells in spleens of mice. Cells were stimulated with anti-CD3 Ab, anti-CD28 Ab, anti-IFN-γ Ab, and IL-4 for 3 days. Values are means ± SEMs from three independent experiments.
ns, not significant.
*p<0.05, **p<0.01, and ***p<0.001.

The STING pathway is activated and the production of IL-4 and IFN-α is increased in CD4⁺ T cells from BLM-treated SKG mice *in vivo*

The numbers of pSTING-producing CD4⁺ T cells, pSTAT6-producing CD4⁺ T cells, and pIRF3-producing CD4⁺ T cells were higher among splenocytes from BLM-treated SKG mice than BLM-treated BALB/c mice (**Fig. 3A** and **Supplementary Fig. 2A**). The number of pSTING, pSTAT6, and pIRF3 of CD4⁺ T cells in spleen tissue were increased in BLM-treated SKG mice (**Fig. 3B**). In addition, the numbers of IFN-α⁺CD4⁺ T cells and IL-4- and IFN-α-producing CD4⁺ T cells among splenocytes were in BLM-treated SKG mice than in BLM-treated BALB/c mice according to flow cytometry and immunofluorescence (**Fig. 3C, D**, and **Supplementary Fig. 2B**). Immunofluorescence showed that STING was activated and translocated to the

https://doi.org/10.4110/in.2024.24.e37

Golgi apparatus in splenocytes of BLM-treated SKG mice (**Fig. 3E**). Next, skin tissue was stained and subjected to immunohistochemistry and immunofluorescence analysis. pSTING, pSTAT6, and pIRF3 were significantly increased in the skin tissue of BLM-treated SKG mice (**Fig. 3F**). Immunofluorescence revealed more IL-4- and IFN-α-producing $CD4^+$ T cells in the skin of BLM-treated SKG mice than in BLM-treated BALB/c mice (**Fig. 3G**).

IL-4 and IFN-α induced fibrosis via the STING pathway, and inhibition of STING reduced fibroblast fibrosis and the production of IL-4 and IFN-α from CD4+ T cells

We treated skin fibroblasts with IL-4 and IFN-α to confirm the effects of IL-4 and IFN-α on skin fibroblasts. As a results, the expression of α-SMA and fibronectin (fibrosis markers) and pSTING, pSTAT6, and pIRF3 in human skin fibroblasts were increased by IL-4 and IFN-α treatment (**Fig. 4A**). Further, the expression of pSTING, pSTAT6, pIRF3, and fibrosis markers were suppressed by H-151 (STING inhibitor). Therefore, IL-4 and IFN-α increase fibrosis by increasing pSTING, pSTAT6, and pIRF3 expression in skin fibroblasts. In addition, to assess the effects of STING on the expression of IL-4 and IFN-α in $CD4^+$ T cells, we differentiated splenocytes from BALB/c and SKG mice under Th2-skewing conditions in the absence or presence of H-151. The numbers of pSTAT6- and pIRF3-expressing $CD4^+$ T cells and IL-4- and IFN-α-producing $CD4^+$ T cells were increased in SKG mice compared to BALB/c mice, an effect reversed by STING inhibition (**Fig. 4B and C**, **Supplementary Fig. 3A and B**). We further confirmed whether fibrosis was inhibited when H-151 was administered to BLM-treated SKG mice. As a result, dermal thickness and the numbers of α-SMA- and Col1-positive cells in skin tissue were reduced by treatment with H-151 (**Fig. 4D and E**). Additionally, it was confirmed that pSTING, pSTAT6, and pIRF3 were decreased in skin tissue by H-151 treatment (**Fig. 4F**).

Inhibition of STAT6 reduced skin fibrosis and the production of IL-4 and IFN-α from CD4+ T cells

Next, to assess the role of STAT6 (downstream of STING), we injected AS1517499 (STAT6 inhibitor) into BLM-treated mice. Inhibition of STAT6 reduced dermal thickness and decreased the numbers of α-SMA- and Col1-positive cells in skin tissue (**Fig. 5A and B**). In addition, there were fewer Th2, and IFN-α^+CD4^+ T cells, as well as IL-4- and IFN-α-producing $CD4^+$ T cells, among splenocytes in SS mice after STAT6 inhibition (**Fig. 5C**). Moreover, the number of Th2 and IL-4- and IFN-α-producing $CD4^+$ T cells was reduced by the STAT6 inhibitor *in vitro* (**Fig. 5D**). Therefore, the STING and STAT6 pathways are potential therapeutic targets in scleroderma.

IL-4- and IFN-α-producing $CD4^+$ T cells in a humanized SS mice model

We found that the expression of pSTING and IL-4- and IFN-α-producing $CD4^+$ T cells were higher in T cells from SS patients compared to HC (**Supplementary Fig. 4**). To investigate the role of human T cells in SS pathogenesis, we designed a humanized SS mouse model using PBMCs from a patient with SS. We injected PBMCs from the patient into NSG mice, which lack functional/mature T, B, and NK cells (**Fig. 6A**). H&E staining revealed that skin thickness was increased in humanized SS mice compared to BLM-treated NSG mice (**Fig. 6B**). α-SMA and Col1 immunohistochemistry showed that skin fibrosis was significantly increased in humanized SS mice (**Fig. 6C**). Also, pSTING, pSTAT6, and pIRF3 were significantly increased in the skin tissue of humanized SS mice (**Fig. 6D**). In addition, IL-4- and IFN-α-producing human $CD4^+$ T cells were identified among splenocytes from humanized SS mice (**Fig. 5E**). Further, immunofluorescence detected IL-4- and IFN-α-producing human $CD4^+$ T cells in the skin of the humanized SS mouse model (**Fig. 5F**). These results suggest that IL-4- and IFN-α-producing CD4+ T cells are identified in the patient with SS and that they contribute to inducing SS.

https://doi.org/10.4110/in.2024.24.e37

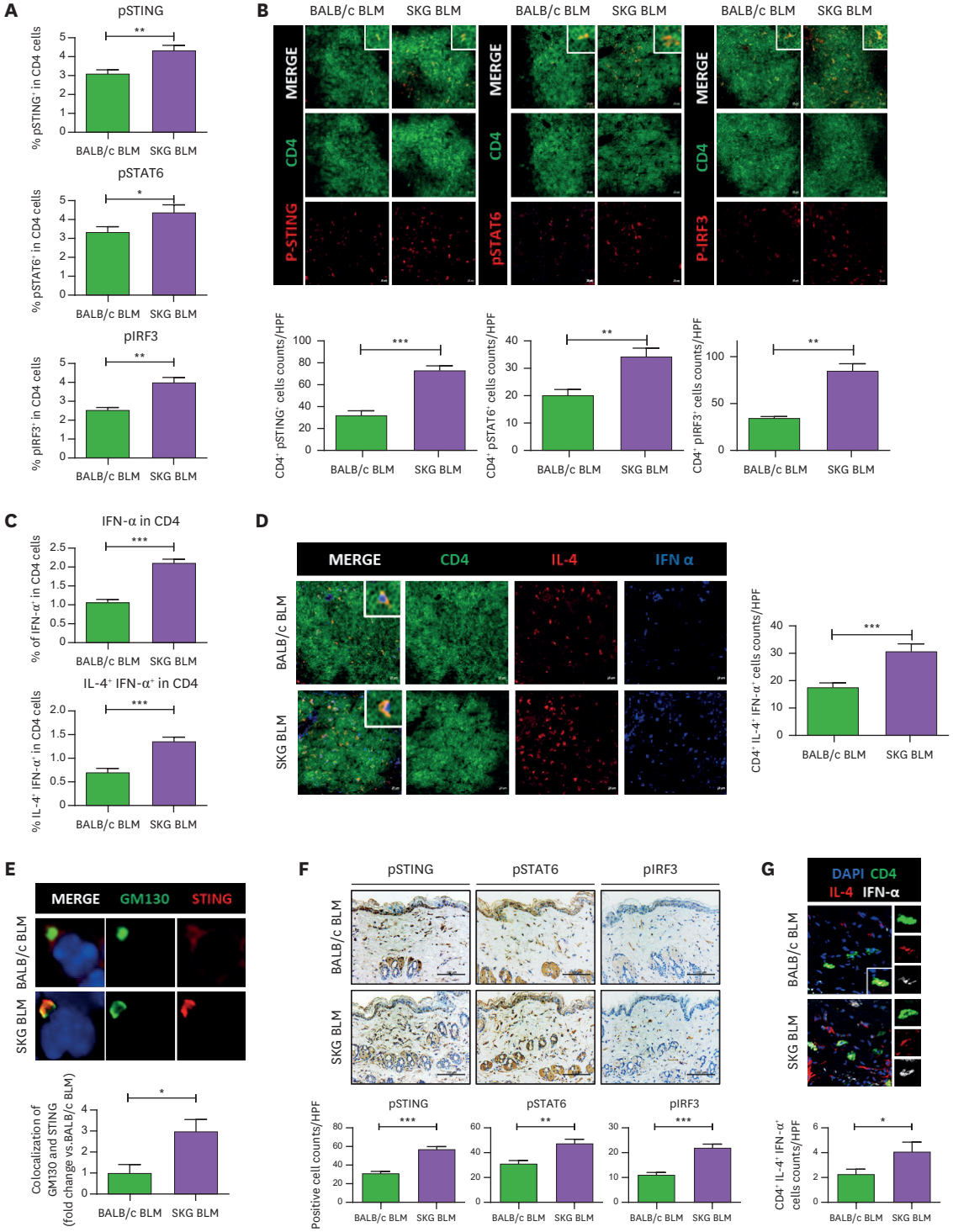

Figure 3. The STING pathway is activated and the production of IL-4 and IFN-α is increased in CD4⁺ T cells from BLM-treated SKG mice *in vivo*. (A) Numbers of pSTING⁺ cells, pSTAT6⁺ cells, and pIRF3⁺ cells among CD4⁺ T cells from spleens of BLM-treated BALB/c mice (n=5) and SKG mice (n=4). (B) Spleen tissues of BLM-treated mice were stained with anti-CD4 (green), anti-pSTING (red), anti-pSTAT6 (red), and anti-pIRF3 (red) Abs. Scale bars=20 μm. (C) Numbers of IFN-α⁺ cells and IL-4⁺ IFN-α⁺ cells among CD4⁺ T cells from spleens of BLM-treated BALB/c mice (n=5) and SKG mice (n=4). (D) Spleen tissues of BLM-treated mice stained with anti-CD4 (green), anti-IL-4 (red), and anti-IFNα (blue) Abs. Scale bars=20 μm. (E) Splenocytes from spleen tissues of BLM-treated mice stained with anti-GM130 (green) and anti-STING (red) Abs. Scale bars=20 μm. (F) Immunohistochemistry of pSTING, pSTAT6, and pIRF3 in skin tissues in BLM-treated mice. Scale bars=100 μm. (G) Representative immunofluorescence images of CD4 (green), IL-4 (red), IFN-α (white), and DAPI (blue) in skin tissues from BLM-treated mice. Scale bars=20 μm. Values are means ± SEMs from three independent experiments.
GM130, Golgi matrix protein 130.
*p<0.05, **p<0.01, and ***p<0.001.

https://doi.org/10.4110/in.2024.24.e37

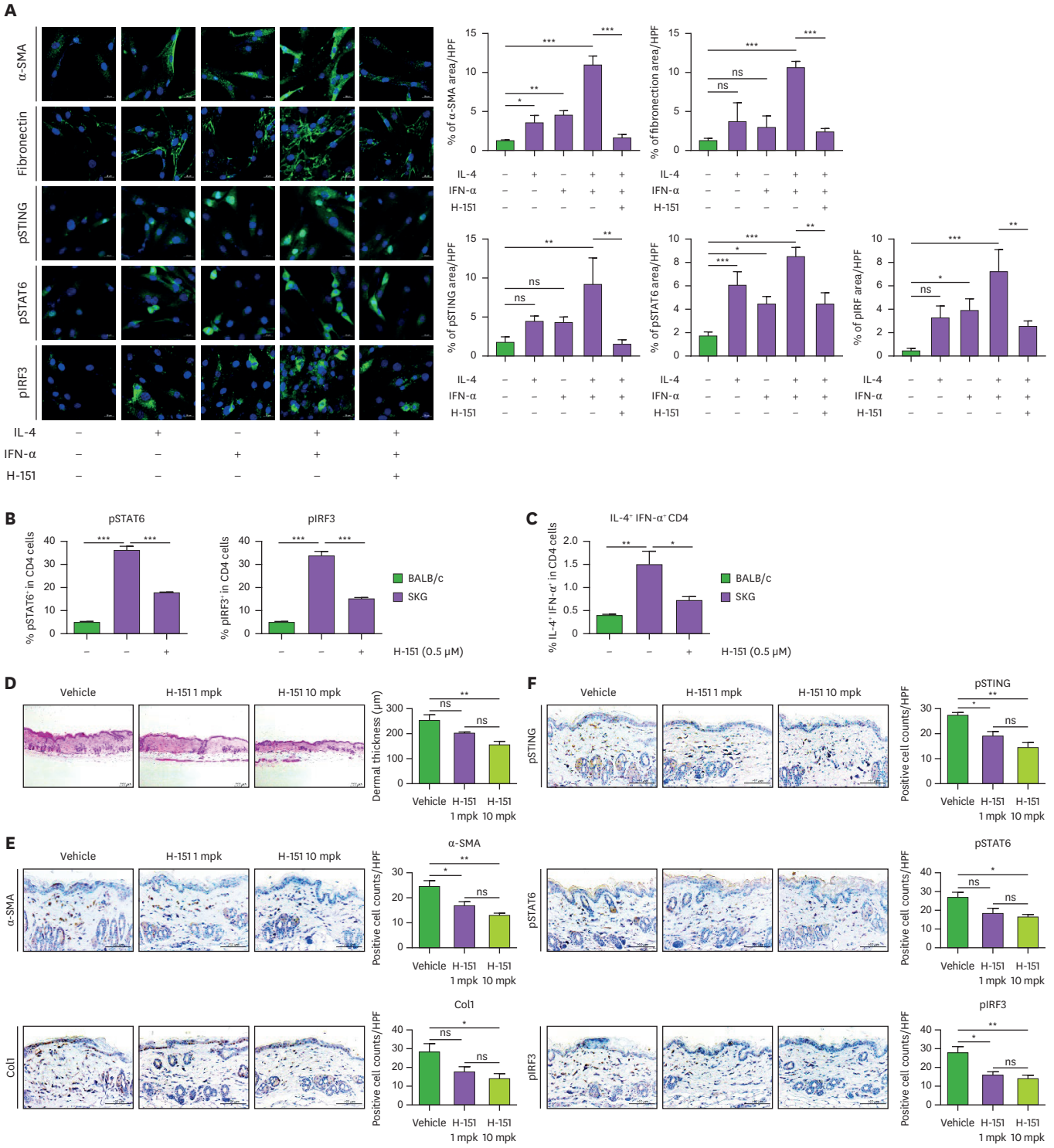

Figure 4. IL-4 and IFN-α induced fibrosis via the STING pathway, and inhibition of STING reduced fibroblast fibrosis and the production of IL-4 and IFN-α from $CD4^+$ T cells. (A) Skin fibroblasts stained with anti-a-SMA (green), anti-fibronectin (green), anti-pSTING (green), anti-pSTAT6 (green) and anti-pIRF3 (green) Abs. Scale bars=20 μm. Skin fibroblasts were stimulated with/without IL-4, IFN-α, and H-151 for 1 days. (B) Numbers of $pSTAT6^+$ cells, $pIRF3^+$ cells, (C) $IL\text{-}4^+$ cells, $IFN\text{-}\alpha^+$ cells, and $IL\text{-}4^+$ $IFN\text{-}\alpha^+$ cells among $CD4^+$ T cells isolated from the spleens of mice. Cells were stimulated with anti-CD3 Ab, anti-CD28 Ab, anti-IFN-γ Ab, and IL-4 with/without H-151 for 3 days. Values are means ± SEMs from three independent experiments.
*p<0.05, **p<0.01, and ***p<0.001.

https://doi.org/10.4110/in.2024.24.e37

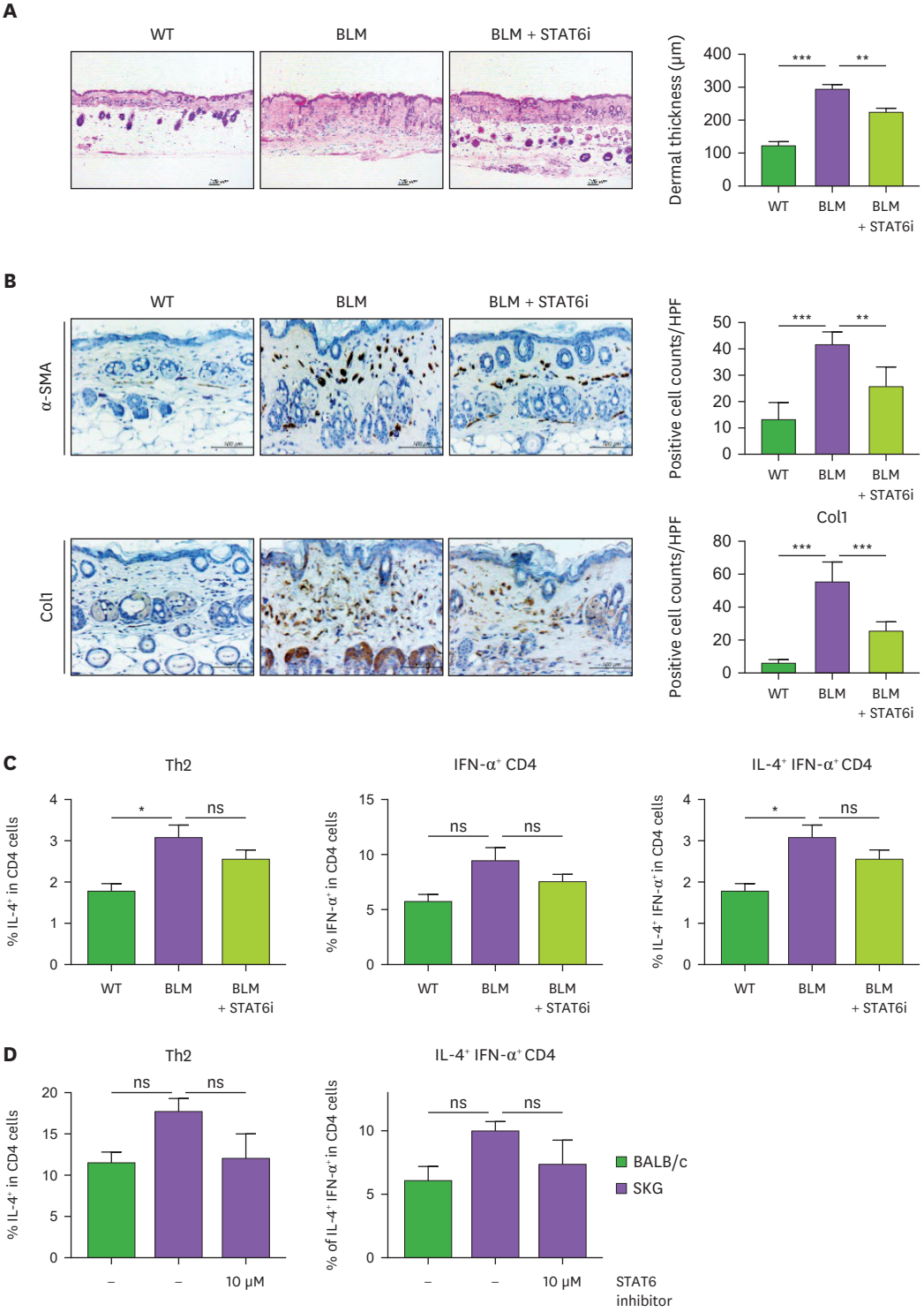

Figure 5. Inhibition of STAT6 reduced skin fibrosis and the production of IL-4 and IFN-α from $CD4^+$ T cells. (A) H&E staining of skin tissue. The mice were given daily subcutaneous injections of BLM for 2 wk. Next, 10 mg/kg AS1517499, a STAT6 inhibitor, was subcutaneously injected three times a week for 3 wk (wild type [n=3], BLM-treated mice [n=5] and BLM and STAT6 inhibitor-treated mice [n=5]). Scale bars=100 μm. (B) Representative α-SMA- and Col1-stained images of skin tissues. Scale bars=100 μm. (C) Numbers of $CD4^+IL\text{-}4^+$ (Th2), IFN-α^+ $CD4^+$ T cells, and IL-4^+ IFN-α^+ cells among $CD4^+$ T cells from the spleens of mice. (D) Numbers of IL-4^+ cells and IL-4^+ IFN-α^+ cells among $CD4^+$ T cells isolated from the spleens of mice. Cells were stimulated with anti-CD3 Ab, anti-CD28 Ab, anti-IFN-γ Ab, and IL-4 with/without AS1517499 for 3 days. Values are means ± SEMs from three independent experiments.
WT, wild type; STAT6 i, STAT6 inhibitor.
*p<0.05, **p<0.01, and ***p<0.001.

https://doi.org/10.4110/in.2024.24.e37

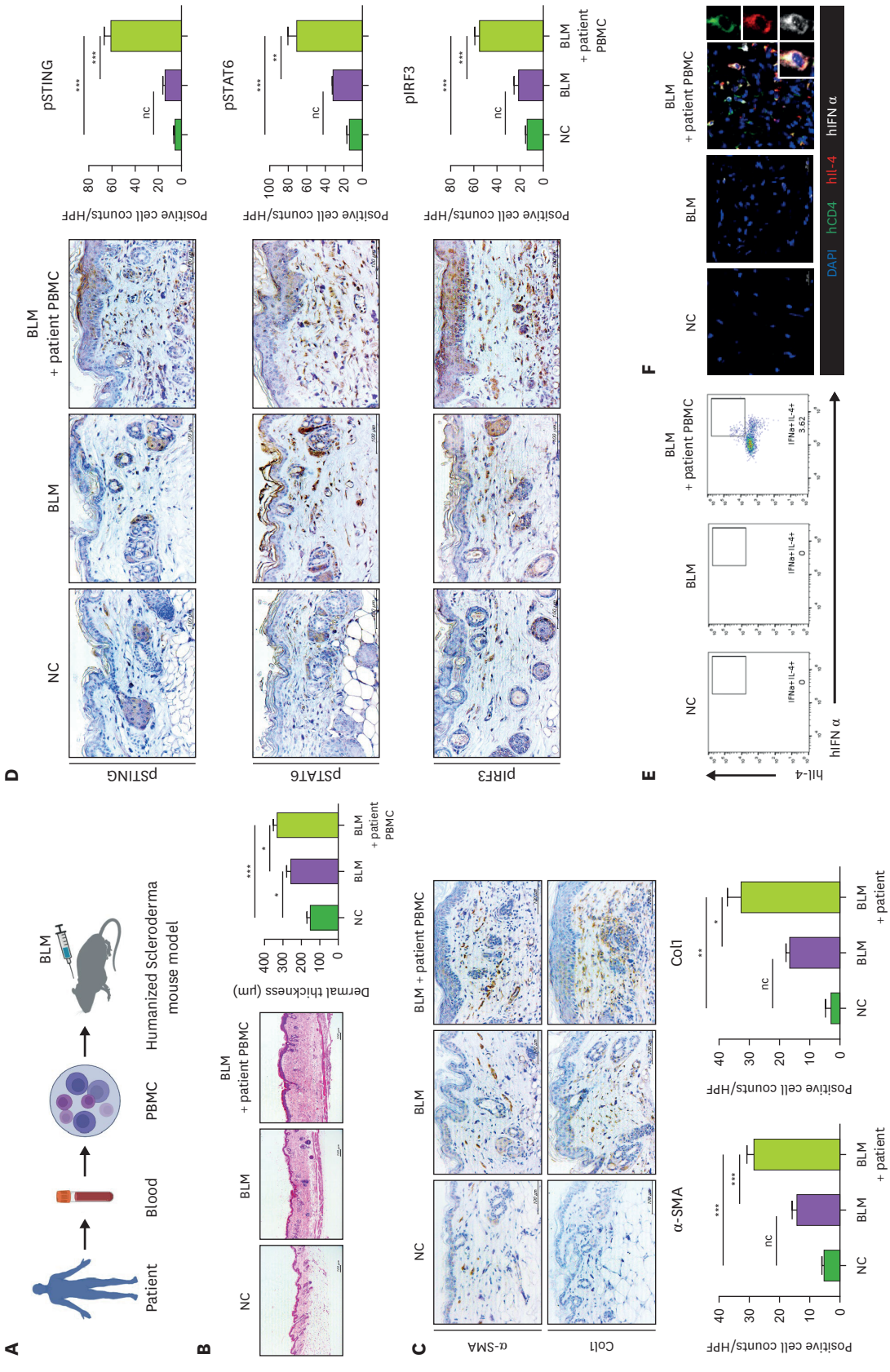

Figure 6. IL-4- and IFN-α-producing CD4$^+$ T cells in a humanized SS mouse model. (A) A patient-derived humanized SS mouse model was developed by injecting human PBMCs and BLMs into NSG mice (normal control [n=3], BLM-treated mice [n=3] and BLM and patient PBMC-treated mice [n=5]). (B) H&E staining of skin tissues from the humanized SS mouse model. Scale bars=100 μm. (C) Representative α-SMA- and Col1-stained images of skin tissues of the humanized SS mouse model. Scale bars=100 μm. (D) Immunohistochemistry of pSTING, pSTAT6, and pIRF3 in skin tissues of the humanized SS mouse model. Scale bars=100 μm. (E) Numbers of IL-4$^+$ IFN-α$^+$ CD4$^+$ T cells in spleen of the humanized SS mouse model. (F) Representative immunofluorescence images of CD4 (green), IL-4 (red), IFN-α (white), and DAPI (blue) in skin tissues from the humanized SS mouse model. Scale bars=20 μm. Values are means ± SEMs from three independent experiments.
hIl-4, human IL-4; hIFN α, human IFN α.
*p<0.05, **p<0.01, and ***p<0.001.

https://doi.org/10.4110/in.2024.24.e37

DISCUSSION

SS is an autoimmune disease involving skin thickening, fibrosis, and vasculopathy (1). SS is categorized as limited or diffuse, which refers to the degree of skin involvement (25). Both types can involve problems in other organs. It has a high mortality rate because of organ-based complications including pulmonary arterial hypertension, lung fibrosis, renal failure, and gastrointestinal tract dysfunction (26).

T-cell activation is significantly associated with SS (27). There are greater numbers of Th2 cells and Th17 cells in the skin and blood of SS patients (6-8). IL-4 concentrations are also higher in serum and PBMCs (28). IL-4 stimulates fibroblast proliferation and their differentiation to myofibroblasts, increasing the production of extracellular matrix and collagen and playing a key role in the development of fibrosis (29,30). $CD4^+$ $CD8^+$ double-positive T cells produce a high level of IL-4, which may enhance extracellular matrix deposition by fibroblasts in SS skin (31). Monocyte chemoattractant protein 1 (MCP-1) stimulates IL-4 synthesis in SS fibroblasts, significantly increasing the production of collagen in SS dermal fibroblasts (32). In a putative murine model of scleroderma, stimulation of IL-4 with Tsk/+ fibroblasts increased type I collagen secretion by these cells, and anti-IL-4 treatment prevented the development of dermal fibrosis (33). Moreover, IL-4 promotes the biogenesis of collagen proteins in SS fibroblasts by increasing the stability and transcription of type 1 and 3 procollagens, and fibronectin (28,34). Thus, IL-4 not only activates fibroblasts to increase the production of extracellular matrix and collagen proteins but also regulates the expression of a-SMA and collagen genes. IL-17A is a pro-inflammatory cytokine produced by Th17 cells and natural killer cells (35). The IL-17 mRNA level is elevated in lesional skin and PBMCs of SS patients (36). In murine models, IL-17A induces fibrosis by promoting fibroblast proliferation and inducing the synthesis of TGF-β, collagen, and connective tissue growth factor (CTGF) (37). In humans, IL-17A induces pro-inflammatory cytokine synthesis and inhibits that of collagen and CTGF, thus having pro-inflammatory and anti-fibrotic effects (38). Therefore, the pro-fibrotic mechanisms of IL-17A in animal models cannot be extrapolated to humans (35).

SKG mice spontaneously develop T cell-mediated autoimmune arthritis. To investigate the role of T cells in SS, we injected BLM into SKG mice, which developed thicker skin and more fibrosis than BLM-treated BALB/c mice. In addition, there were more Th2 and Th17 cells in blood and the levels of cytokines related to SS were elevated in skin lesions of BLM-treated SKG, as in patients with SS. Our data indicate that the increased numbers of inflammatory T cells caused by the mutation of ZAP70 can induce SS, thus showing potential as a therapeutic target.

STIM1, a key component of SOCE, regulates STING activity via physical interactions under resting conditions (12). Activated STIM1 translocates from the ER membrane to the PM, where it dissociates from and thereby activates STING. Dissociation of STIM1 and STING triggers the production of type I IFN and inflammatory cytokines by activating IRF3 and STAT6. We found that STIM1 is activated in T cells from SKG mice, which activates STING signaling. Also, when the STIM1–STING axis is activated, it induces the production of type I IFN and IL-4 and accelerates the development and progression of SS. In this study, activation of STIM1 by the ZAP70 mutation led to the dissociation and activation of STING. Activating STING in SKG mice induced the production of type I IFN and IL-4 and increased disease severity in BLM-induced SKG mice compared to BALB/c mice. This is the first report that STING-induced production of type I IFN and IL-4 in T cells is implicated in the development

and progression of SS. Although T cells have been reported to express type I IFN and IL-4, there are no reports of T cells expressing them simultaneously (6,39). These two cytokines are known to be cytokines that increase fibrosis (30,40). We confirmed that IL-4- and IFN-α-producing $CD4^+$ T cells were infiltrated in the dermis of skin tissue in the SS mouse model in which fibrosis was induced (**Figs. 3G** and **6F**). To determine whether IL-4- and IFN-α-producing $CD4^+$ T cells affect fibrosis, human skin fibroblasts were treated with IL-4- and IFN-α alone or in combination. As a result, it was confirmed that the expression of fibrosis markers increased statistically significantly in the group treated with the combination treatment compared to the single treatment group (**Fig. 4A**). Through this, it was found that that IL-4- and IFN-α-producing CD4+ T cells through STING activation strongly promote the progression of tissue fibrosis. Therefore, targeting these cells is thought to be important in the treatment of not only SS but also other autoimmune diseases related to fibrosis. IFN-regulated genes are expressed in the peripheral blood and skin of patients with SS (41). STAT6 induces the expression of IL-4 in T cells and is a transcription factor involved in collagen production by fibroblasts (42,43). STING has been studied in mainly dendritic cells (DCs) or macrophages. We demonstrate the pathophysiological role of STING in T cells on the SS. Our data provide the possibility of STING as the therapeutic target not only in DCs or macrophages but also T cells.

Previously, we have established a humanized animal model of SS (24). In this study, we used a humanized SS mouse model which represents the pathophysiology of human SS patients better than the mouse SS model. It was confirmed that the expression of pSTING in $CD4^+$ T cells and the number of IL-4- and IFN-α-producing $CD4^+$ T cells were increased in SS patients compared to healthy controls (**Supplementary Fig. 4**). The results showed enhanced fibrosis and the production of type I IFN and IL-4 in skin of humanized SS mouse model compared to skin of BLM-treated NSG mice.

Therefore, STING-induced type I IFN and IL-4 production is implicated in the development and progression of SS in not only mice but also humans. Our data from humanized SS mouse model provide the strong evidence that STING is one of the candidates for SS treatment. Also, our data suggest that STAT6 is another therapeutic target of SS by regulating IL-4 expression.

Taken together, we found the crucial role of STING in the development and progression of SS. Our data suggest that STING-induced production of IL-4- and type I IFN by $CD4^+$ T cells is a key factor in mouse model and humanized mouse model of SS. Therefore, STING is a potential therapeutic target in SS.

ACKNOWLEDGEMENTS

This research was supported by Korea Drug Development Fund funded by Ministry of Science and ICT, Ministry of Trade, Industry, and Energy, and Ministry of Health and Welfare (RS-2023-00217274, Republic of Korea) and a grant of the Korea Health Technology R&D Project through the Korea Health Industry Development Institute (KHIDI), funded by the Ministry of Health & Welfare, Republic of Korea (grant number: RS-2022-KH127879[HV22C0069]).

SUPPLEMENTARY MATERIALS

Supplementary Figure 1

The representative flow cytometry plots. The representative flow cytometry plots of pSTING$^+$ cells, pSTAT6$^+$ cells, pIRF3$^+$ cells, and IL-4$^+$ IFN-α$^+$ cells of CD4$^+$ T cells in spleens of mice. Cells were stimulated with anti-CD3 Ab, anti-CD28 Ab, anti-IFN-γ Ab, and IL-4 for 3 days.

Supplementary Figure 2

The representative flow cytometry plots. (A) The representative flow cytometry plots of pSTING$^+$ cells, pSTAT6$^+$ cells, and pIRF3$^+$ cells among CD4$^+$ T cells from spleens of BLM-treated BALB/c mice (n=5) and SKG mice (n=4). (B) The representative flow cytometry plots of IFN-α$^+$ cells and IL-4$^+$ IFN-α$^+$ cells among CD4$^+$ T cells from spleens of BLM-treated BALB/c mice (n=5) and SKG mice (n=4).

Supplementary Figure 3

The representative flow cytometry plots. The representative flow cytometry plots of (A) pSTAT6$^+$ cells, pIRF3$^+$ cells and (B) IL-4$^+$ IFN-α$^+$ cells among CD4$^+$ T cells isolated from the spleens of mice. Cells were stimulated with anti-CD3 Ab, anti-CD28 Ab, anti-IFN-γ Ab, and IL-4 with/without H-151 for 3 days.

Supplementary Figure 4

Expression levels of pSTING and IL-4- and IFN-α-producing CD4$^+$ T cells in SS patients. The numbers of pSTING$^+$ cells and IL-4$^+$ IFN-α$^+$ cells among CD4$^+$ T cells from the PBMCs of HC (n=4) and SS patients (n=3).

REFERENCES

1. Boleto G, Allanore Y, Avouac J. Targeting costimulatory pathways in systemic sclerosis. *Front Immunol* 2018;9:2998. PUBMED | CROSSREF
2. Castello-Cros R, Whitaker-Menezes D, Molchansky A, Purkins G, Soslowsky LJ, Beason DP, Sotgia F, Iozzo RV, Lisanti MP. Scleroderma-like properties of skin from caveolin-1-deficient mice: implications for new treatment strategies in patients with fibrosis and systemic sclerosis. *Cell Cycle* 2011;10:2140-2150. PUBMED | CROSSREF
3. Almanzar G, Schmalzing M, Klein M, Hilligardt D, Morris P, Höfner K, Hajj NE, Kneitz H, Wild V, Rosenwald A, et al. Memory CD4+ T cells lacking expression of CCR7 promote pro-inflammatory cytokine production in patients with diffuse cutaneous systemic sclerosis. *Eur J Dermatol* 2019;29:468-476. PUBMED | CROSSREF
4. Yamamoto T. Autoimmune mechanisms of scleroderma and a role of oxidative stress. *Self Nonself* 2011;2:4-10. PUBMED | CROSSREF
5. Yap HY, Tee SZ, Wong MM, Chow SK, Peh SC, Teow SY. Pathogenic role of immune cells in rheumatoid arthritis: implications in clinical treatment and biomarker development. *Cells* 2018;7:161. PUBMED | CROSSREF
6. Mavalia C, Scaletti C, Romagnani P, Carossino AM, Pignone A, Emmi L, Pupilli C, Pizzolo G, Maggi E, Romagnani S. Type 2 helper T-cell predominance and high CD30 expression in systemic sclerosis. *Am J Pathol* 1997;151:1751-1758. PUBMED
7. Radstake TR, van Bon L, Broen J, Hussiani A, Hesselstrand R, Wuttge DM, Deng Y, Simms R, Lubberts E, Lafyatis R. The pronounced Th17 profile in systemic sclerosis (SSc) together with intracellular expression of TGFbeta and IFNgamma distinguishes SSc phenotypes. *PLoS One* 2009;4:e5903. PUBMED | CROSSREF
8. Xing X, Yang J, Yang X, Wei Y, Zhu L, Gao D, Li M. IL-17A induces endothelial inflammation in systemic sclerosis via the ERK signaling pathway. *PLoS One* 2013;8:e85032. PUBMED | CROSSREF

9. Brembilla NC, Montanari E, Truchetet ME, Raschi E, Meroni P, Chizzolini C. Th17 cells favor inflammatory responses while inhibiting type I collagen deposition by dermal fibroblasts: differential effects in healthy and systemic sclerosis fibroblasts. *Arthritis Res Ther* 2013;15:R151. PUBMED | CROSSREF
10. Trebak M, Kinet JP. Calcium signalling in T cells. *Nat Rev Immunol* 2019;19:154-169. PUBMED | CROSSREF
11. Woo JS, Srikanth S, Gwack Y. Modulation of Orai1 and STIM1 by cellular factors. In: Calcium Entry Channels in Non-Excitable Cells. Kozak JA, Putney JW Jr, edis. Boca Raton, FL; CRC Press/Taylor & Francis; 2018. p.73-92.
12. Srikanth S, Woo JS, Wu B, El-Sherbiny YM, Leung J, Chupradit K, Rice L, Seo GJ, Calmettes G, Ramakrishna C, et al. The Ca^{2+} sensor STIM1 regulates the type I interferon response by retaining the signaling adaptor STING at the endoplasmic reticulum. *Nat Immunol* 2019;20:152-162. PUBMED | CROSSREF
13. Son A, de Jesus AA, Schwartz DM. STIM1 holds a STING in its (N-terminal) tail. *Cell Calcium* 2019;80:192-193. PUBMED | CROSSREF
14. Tanaka Y, Chen ZJ. STING specifies IRF3 phosphorylation by TBK1 in the cytosolic DNA signaling pathway. *Sci Signal* 2012;5:ra20. PUBMED | CROSSREF
15. Zhang X, Shi H, Wu J, Zhang X, Sun L, Chen C, Chen ZJ. Cyclic GMP-AMP containing mixed phosphodiester linkages is an endogenous high-affinity ligand for STING. *Mol Cell* 2013;51:226-235. PUBMED | CROSSREF
16. Zhao B, Du F, Xu P, Shu C, Sankaran B, Bell SL, Liu M, Lei Y, Gao X, Fu X, et al. A conserved PLPLRT/SD motif of STING mediates the recruitment and activation of TBK1. *Nature* 2019;569:718-722. PUBMED | CROSSREF
17. Liu S, Cai X, Wu J, Cong Q, Chen X, Li T, Du F, Ren J, Wu YT, Grishin NV, et al. Phosphorylation of innate immune adaptor proteins MAVS, STING, and TRIF induces IRF3 activation. *Science* 2015;347:aaa2630. PUBMED | CROSSREF
18. Chen H, Sun H, You F, Sun W, Zhou X, Chen L, Yang J, Wang Y, Tang H, Guan Y, et al. Activation of STAT6 by STING is critical for antiviral innate immunity. *Cell* 2011;147:436-446. PUBMED | CROSSREF
19. Santana-de Anda K, Gómez-Martín D, Monsivais-Urenda AE, Salgado-Bustamante M, González-Amaro R, Alcocer-Varela J. Interferon regulatory factor 3 as key element of the interferon signature in plasmacytoid dendritic cells from systemic lupus erythematosus patients: novel genetic associations in the Mexican mestizo population. *Clin Exp Immunol* 2014;178:428-437. PUBMED | CROSSREF
20. Takeda K, Tanaka T, Shi W, Matsumoto M, Minami M, Kashiwamura S, Nakanishi K, Yoshida N, Kishimoto T, Akira S. Essential role of Stat6 in IL-4 signalling. *Nature* 1996;380:627-630. PUBMED | CROSSREF
21. Hsu LY, Tan YX, Xiao Z, Malissen M, Weiss A. A hypomorphic allele of ZAP-70 reveals a distinct thymic threshold for autoimmune disease versus autoimmune reactivity. *J Exp Med* 2009;206:2527-2541. PUBMED | CROSSREF
22. Sakaguchi N, Takahashi T, Hata H, Nomura T, Tagami T, Yamazaki S, Sakihama T, Matsutani T, Negishi I, Nakatsuru S, et al. Altered thymic T-cell selection due to a mutation of the ZAP-70 gene causes autoimmune arthritis in mice. *Nature* 2003;426:454-460. PUBMED | CROSSREF
23. Hata H, Sakaguchi N, Yoshitomi H, Iwakura Y, Sekikawa K, Azuma Y, Kanai C, Moriizumi E, Nomura T, Nakamura T, et al. Distinct contribution of IL-6, TNF-alpha, IL-1, and IL-10 to T cell-mediated spontaneous autoimmune arthritis in mice. *J Clin Invest* 2004;114:582-588. PUBMED | CROSSREF
24. Park MJ, Park Y, Choi JW, Baek JA, Jeong HY, Na HS, Moon YM, Cho ML, Park SH. Establishment of a humanized animal model of systemic sclerosis in which T helper-17 cells from patients with systemic sclerosis infiltrate and cause fibrosis in the lungs and skin. *Exp Mol Med* 2022;54:1577-1585. PUBMED | CROSSREF
25. Derk CT, Jimenez SA. Systemic sclerosis: current views of its pathogenesis. *Autoimmun Rev* 2003;2:181-191. PUBMED | CROSSREF
26. Denton CP, Black CM. Scleroderma--clinical and pathological advances. *Best Pract Res Clin Rheumatol* 2004;18:271-290. PUBMED | CROSSREF
27. O'Reilly S, Hügle T, van Laar JM. T cells in systemic sclerosis: a reappraisal. *Rheumatology (Oxford)* 2012;51:1540-1549. PUBMED | CROSSREF
28. Famularo G, Procopio A, Giacomelli R, Danese C, Sacchetti S, Perego MA, Santoni A, Tonietti G. Soluble interleukin-2 receptor, interleukin-2 and interleukin-4 in sera and supernatants from patients with progressive systemic sclerosis. *Clin Exp Immunol* 1990;81:368-372. PUBMED | CROSSREF
29. Wynn TA. Fibrotic disease and the T(H)1/T(H)2 paradigm. *Nat Rev Immunol* 2004;4:583-594. PUBMED | CROSSREF
30. Salmon-Ehr V, Serpier H, Nawrocki B, Gillery P, Clavel C, Kalis B, Birembaut P, Maquart FX. Expression of interleukin-4 in scleroderma skin specimens and scleroderma fibroblast cultures. Potential role in fibrosis. *Arch Dermatol* 1996;132:802-806. PUBMED | CROSSREF

31. Parel Y, Aurrand-Lions M, Scheja A, Dayer JM, Roosnek E, Chizzolini C. Presence of CD4+CD8+ double-positive T cells with very high interleukin-4 production potential in lesional skin of patients with systemic sclerosis. *Arthritis Rheum* 2007;56:3459-3467. PUBMED | CROSSREF
32. Distler JH, Jüngel A, Caretto D, Schulze-Horsel U, Kowal-Bielecka O, Gay RE, Michel BA, Müller-Ladner U, Kalden JR, Gay S, et al. Monocyte chemoattractant protein 1 released from glycosaminoglycans mediates its profibrotic effects in systemic sclerosis via the release of interleukin-4 from T cells. *Arthritis Rheum* 2006;54:214-225. PUBMED | CROSSREF
33. Ong C, Wong C, Roberts CR, Teh HS, Jirik FR. Anti-IL-4 treatment prevents dermal collagen deposition in the tight-skin mouse model of scleroderma. *Eur J Immunol* 1998;28:2619-2629. PUBMED | CROSSREF
34. Lee KS, Ro YJ, Ryoo YW, Kwon HJ, Song JY. Regulation of interleukin-4 on collagen gene expression by systemic sclerosis fibroblasts in culture. *J Dermatol Sci* 1996;12:110-117. PUBMED | CROSSREF
35. Chizzolini C, Dufour AM, Brembilla NC. Is there a role for IL-17 in the pathogenesis of systemic sclerosis? *Immunol Lett* 2018;195:61-67. PUBMED | CROSSREF
36. Kurasawa K, Hirose K, Sano H, Endo H, Shinkai H, Nawata Y, Takabayashi K, Iwamoto I. Increased interleukin-17 production in patients with systemic sclerosis. *Arthritis Rheum* 2000;43:2455-2463. PUBMED | CROSSREF
37. Wilson MS, Madala SK, Ramalingam TR, Gochuico BR, Rosas IO, Cheever AW, Wynn TA. Bleomycin and IL-1beta-mediated pulmonary fibrosis is IL-17A dependent. *J Exp Med* 2010;207:535-552. PUBMED | CROSSREF
38. Gonçalves RS, Pereira MC, Dantas AT, Almeida AR, Marques CD, Rego MJ, Pitta IR, Duarte AL, Pitta MG. IL-17 and related cytokines involved in systemic sclerosis: Perspectives. *Autoimmunity* 2018;51:1-9. PUBMED | CROSSREF
39. Simpson SR, Rego SL, Harvey SE, Liu M, Hemphill WO, Venkatadri R, Sharma R, Grayson JM, Perrino FW. T cells produce IFN-α in the TREX1 D18N model of lupus-like autoimmunity. *J Immunol* 2020;204:348-359. PUBMED | CROSSREF
40. Ding X, Ren Y, He X. IFN-I mediates lupus nephritis from the beginning to renal fibrosis. *Front Immunol* 2021;12:676082. PUBMED | CROSSREF
41. Skaug B, Assassi S. Type I interferon dysregulation in Systemic Sclerosis. *Cytokine* 2020;132:154635. PUBMED | CROSSREF
42. Kippenberger S, Zöller N, Kleemann J, Müller J, Kaufmann R, Hofmann M, Bernd A, Meissner M, Valesky E. STAT6-dependent collagen synthesis in human fibroblasts is induced by bovine milk. *PLoS One* 2015;10:e0131783. PUBMED | CROSSREF
43. Nguyen JK, Austin E, Huang A, Mamalis A, Jagdeo J. The IL-4/IL-13 axis in skin fibrosis and scarring: mechanistic concepts and therapeutic targets. *Arch Dermatol Res* 2020;312:81-92. PUBMED | CROSSREF